Band Gap Tuning in Nanoporous TiO_2-ZrO_2 Hybrid Thin Films

Chang-Sik Kim and Hyun-Dam Jeong*

*Department of Chemistry, Chonnam National University, Gwangju 500-575, Korea. *E-mail: hdjeong@chonnam.ac.kr*
Received September 17, 2007

Nanoporous TiO_2 and ZrO_2 thin films were spin-coated using a surfactant-templated approach from Pluronic P123 ($EO_{20}PO_{70}EO_{20}$) as the templating agent, titanium alkoxide ($Ti(OC_4H_9)_4$) as the inorganic precursor, and butanol as a the solvent. The control of the electronic structure of TiO_2 is crucial for its various applications. We found that the band gap of the hybrid nanoporous thin films can be easily tuned by adding an acetylacetone-stabilized $Zr(OC_4H_9)_4$ precursor to the precursor solution of $Ti(OC_4H_9)_4$. Pores with a diameter of 5 nm-10 nm were randomly dispersed and partially connected to each other inside the films. TiO_2 and ZrO_2 thin films have an anatase structure and tetragonal structure, respectively, while the TiO_2-ZrO_2 hybrid film exhibited no crystallinity. The refractive index was significantly changed by varying the atomic ratio of titanium to zirconium. The band gap for the nanoporous TiO_2 was estimated to 3.43 eV and that for the TiO_2-ZrO_2 hybrid film was 3.61 eV.

Key Words : Nanoporous, TiO_2, ZrO_2, Thin film, Band gap

Introduction

Thin films of metal oxides have been of great interest because of their essential roles in electronic, electrical, optical and magnetic applications. Among these films, TiO_2 thin films have been studied intensively, since they have diverse applications such as optoelectronic devices,[1] photocatalysts,[2,3] antireflection coatings for silicon solar cells[4] and photoanode materials for dye-sensitized solar cells (DSSC).[5,6] Recently, the TiO_2 thin films have been regarded as potential high dielectric constant materials (high-k) for DRAM with an extremely small feature (<100 nm).[7,8] They have also been receiving attracting interest as transistor gate dielectrics in complementary metal-oxide semiconductor (CMOS) field-effect transistor (FET) logic devices, and as the transistor gate dielectrics in thin film transistor (TFT) display devices.[9] In addition to TiO_2 films, ZrO_2 ones has been also regarded as another high-k candidate for the semiconductor and display industry, because of their high dielectric constant of about 25, high melting point of 2700 °C, and excellent chemical stability.[10-12]

A number of methods have been employed to deposit oxide films, including e-beam evaporation, sputtering, chemical vapor deposition, and the sol-gel process.[13] The sol-gel process is one of the most practical solution-deposition methods of preparing oxide thin films. The use of the sol-gel process, in which a sol solution of inorganic precursors is mostly spin-coated, is believed to have several advantages, good homogeneity, ease of composition control, low processing temperature, large area coating, low equipment cost and good optical properties. Especially, it has considerable potential to be combined with the newly emerging techniques of nano-chemistry, thereby allowing innovations to be made for various applications. Among these, the surfactant-templated approach has drawn much interest as a new next-generation concept for synthesizing nanoporous oxide thin films.[14,15] Nanoporous titanium oxide has been investigated extensively because of its many potential applications; in particular, its application to the photoanode materials of DSSC is very promising.[6] This is because its high surface area increases the amount of dye adsorbed, allowing a higher current density in the cell operation.

In this study, we mainly focused on the band gap tuning of nanoporous TiO_2 thin films synthesized using the surfactant-templated approach. The control of the band gap was realized by incorporating the molecular structure of ZrO_2 into the solid networks of the nanoporous TiO_2 thin films.

Experimental Section

Synthesis of TiO_2 precursor solution. All reaction were performed at room temperature 1.57 g of $Ti(OC_4H_9)_4$ (titanium(IV) butoxide, reagent grade, 97%) was dissolved in 1 g of *n*-butanol, and 0.8 g of HCl (hydrochloric acid, 35%) was added slowly under vigorous stirring at room temperature. 0.57 g of poly(ethylene oxide)-poly(propylene oxide)-poly(ethylene oxide) block copolymer $EO_{20}PO_{70}EO_{20}$ (Pluronic P123, BASF) was dissolved in 3 g of *n*-butanol and stirred at room temperature for 30 min. The P123 solution was mixed with the titanium (IV) butoxide solution and stirred for 3 hr.

Synthesis of ZrO_2 precursor solution. The synthesis of the ZrO_2 precursor solution is somewhat different from that of the TiO_2 precursor solution. Since the reactivity of $Zr(OC_4H_9)_4$ (zirconium(iv) butoxide-80 wt % solution in 1-butanol) is high, using pure $Zr(OC_4H_9)_4$ precursor without a stabilization process gives rise to a gel state when adding HCl (hydrochloric acid, 35%). To lower the reactivity of the $Zr(OC_4H_9)_4$ precursor, $CH_3COCH_2COCH_3$ (acetylacetone, ≥99%) is added to the $Zr(OC_4H_9)_4$ solution. Firstly, 2.2 g of the $Zr(OC_4H_9)_4$ reagent is dissolved in 0.56 g of *n*-butanol and 0.46 g of acetylacetone is added, followed by 5 min of

stirring. 0.8 g of HCl (hydrochloric acid, 35%) is then added slowly under vigorous stirring for 5 min at room temperature. 0.57 g of the poly(ethylene oxide)-poly(propylene oxide)-poly(ethylene oxide) block copolymer $EO_{20}PO_{70}EO_{20}$ (Pluronic P123, BASF) was dissolved in 3 g of *n*-butanol and stirred at room temperature for 30 min. The P123 solution was mixed with the acetylacetone-stabilized the $Zr(OC_4H_9)_4$ solution and stirred for 3 hr.

Synthesis of TiO_2/ZrO_2 precursor solution. 1.1 g of the $Zr(OC_4H_9)_4$ reagent (2.3 mmol of $Zr(OC_4H_9)_4$ molecules) are dissolved in 0.78 g of *n*-butanol and 0.23 g of acetylacetone is added, followed by 5 min of stirring. To this solution, 0.78 g of $Ti(OC_4H_9)_4$ (2.3 mmol of $Ti(OC_4H_9)_4$ molecules) is added, followed by 5 min of stirring. 0.8 g of HCl (hydrochloric acid, 35%) were then added slowly under vigorous stirring at room temperature. 0.57 g of the poly(ethylene oxide)-poly(propylene oxide)-poly(ethylene oxide) block copolymer $EO_{20}PO_{70}EO_{20}$ (Pluronic P123, BASF) of 0.57 g was dissolved in 3 g of butanol and stirred at room temperature for 30 min. The P123 solution was mixed with the titanium butoxide/zirconium butoxide mixed solution and stirred for 3 hr.

Film preparation. After filtering the precursor solutions using a filter with a size of 0.2 μm size, they were spin-coated on a Si-wafer (resistivity: 1-30 Ω·cm, thickness: 525 nm) at 2000 rpm. Then, and the films were heated on an 80 °C hot plate for 1h to remove the solvent. The films were cured at a temperature of 450 °C in a the vacuum of about 1.3 Pa for 1 hr.

Film characterization. To obtain the information of the surface and roughness of the films, after anodization and soaking, field emission SEM (FE-SEM: model JSM-7500F) images were obtained. To investigate the crystallinity of the films, X-ray diffraction (XRD) was used. The diffractometer used was a Rigaku D/max-RC, and the measurement method wsa the 2θ method, where 2θ was in the range of 20-60°, the scan rate 2° a minute, the target Cu, and the power 40 kV, 100 mA. By using X-ray photoelectron spectroscopy (XPS), the chemical compositions of the films were investigated. The measured peaks in high resolution mode were C1s, O1s, Ti 2p, and Zr 3d. The spectroscope used was a Multilab 2000, and Mg Kα was used as the excitation source. The refractive index (n) and non-zero extinction coefficient (k) were obtained using spectroscopic ellipsometry (SE: model M2000).

Results and Discussion

The nanoporous thin films were spin-coated from Pluronic P123 ($EO_{20}PO_{70}EO_{20}$) as the templating agent, titanium butoxide ($Ti(OC_4H_9)_4$) and zirconium butoxide ($Zr(OC_4H_9)_4$) as the inorganic precursor, and butanol as the solvent, as explained in the experimental section. In this way, a TiO_2-ZrO_2 hybrid thin film was obtained from the precursor solution in which the sols were copolymerized from the two inorganic precursors. Figure 1 shows the top view images of the TiO_2, TiO_2-ZrO_2 hybrid, and ZrO_2 thin films obtained using field emission secondary electron microscopy (FE-SEM). For the TiO_2 thin films in Figure 1(a), the size of the pores is mostly in the range of 5 nm-10 nm, with some of the pores being interconnected. The arrangement of the pores does not show any features of an ordered structure, which is not consistent with the results of a previous study using the same sample preparation method.[14] For the TiO_2-ZrO_2 hybrid and ZrO_2 thin films, pores with diameters of 5 nm-10 nm are also observed, but with slightly different pore connectivities.

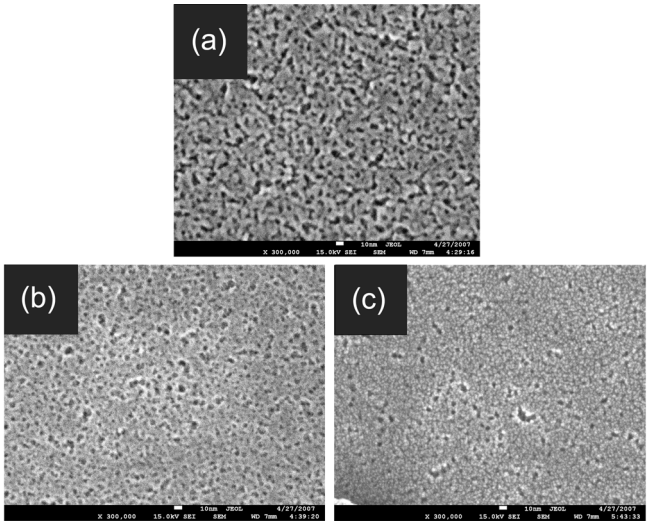

Figure 1. Typical the surface and cross section SEM images of the nanoporous TiO_2-ZrO_2 hybrid film (a) the Nanoporous TiO_2 film (b) the Nanoporous TiO_2-ZrO_2 hybrid film (c) the Nanoporous ZrO_2 film.

The crystallinity of the TiO_2, TiO_2-ZrO_2 hybrid, and ZrO_2 thin films were investigated by using X-ray diffraction (XRD), as shown in Figure 2. The peak intensities for the thin films are weak and especially there are no peaks for the TiO_2-ZrO_2 hybrid thin film, indicating the absence of crystalline domains. The XPD spectrum for the TiO_2 film shows peaks of an anatase structure, where 25.3° and 53.9° correspond to the (101) and (105) indices, respectively. Here, the strong peak at 55.3° is assigned to the (311) plane

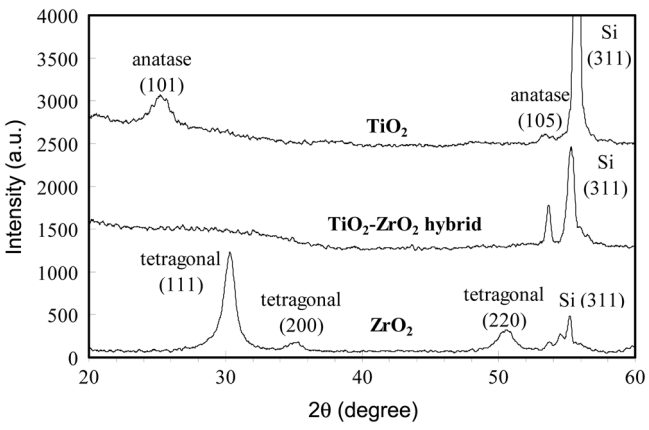

Figure 2. X-Ray Diffraction patterns of TiO_2, TiO_2-ZrO_2 hybrid, ZrO_2 thin films cured at 450 °C.

of the Si substrate. The broadness of the peak of (101) index is related to the size of the hexagonal crystalline phase. The full width at half maximum (FWHM) height of the peak at $2\theta = 25.3^{o}$ was observed to be 1.593 degrees. The Scherrer formula, $t = 0.9\ \lambda/\beta\cos\theta$, where λ is the wavelength of the incident X-rays, β the full width at half maximum height in radians, and θ the diffracted angle, was used to determine the crystalline domain size. The crystalline domain size for the TiO_2 thin film was calculated to be 5.1 nm. From this result, we consider that the film consists of anatase TiO_2 nanocrystalline domains embedded in an amorphous titanium oxide matrix. The ZrO_2 thin film has a somewhat higher crystallinity compared to the other thin films. The peaks which appeared at 30.5^{o}, 35.8^{o}, and 50.9^{o} are attributed to the (111), (200), and (220) planes of the tetragonal crystal structure, respectively. Since the FWHM at 30.5^{o} is 1.250 degrees, the tetragonal crystalline domain size is estimated to be about 6.6 nm. Here, we also believe that the film consists of tetragonal ZiO_2 nanocrystalline domains embedded in an amorphous zirconium oxide matrix. For the TiO_2-ZrO_2 hybrid thin film, no crystallinity was observed, implying that the TiO_2 and ZrO_2 precursors interrupt with each other so as to prevent the formation of the nanocrystalline domains.

Table 1 shows the X-ray photoelectron spectroscopy (XPS) quantification results of the chemical composition of the TiO_2, TiO_2-ZrO_2 hybrid, and ZrO_2 thin films.[16] The atomic concentration of carbon element is observed to be greater than expected, which means that organic residues originating to the P123 surfactant remain inside the films. This is surely because the P123 surfactants are not completely removed at the curing temperature of 450 °C. Although the relative mole ratio of the zirconium precursor to the titanium precursor used in the preparation of the precursor solution is kept at 1.0, the amount of zirconium element in the film is two times greater than that of titanium element in our XPS quantification. It is thought that the reactivity of the $Zr(OC_4H_9)_4$ precursor stabilized with acetylacetone is higher than that of $Ti(OC_4H_9)_4$ precursor and that the zirconium is more easily incorporated in the sol state of the precursor solution.

The thickness, refractive index (n), and non-zero extinction coefficient (k) of the thin films were measured using spectroscopic ellipsometry (SE), which is another efficient way to investigate the film properties. The thicknesses measured for the TiO_2, TiO_2-ZrO_2 and ZrO_2 thin films are 192, 131 and 112 nm, respectively. In the dispersion curve of n shown in Figure 3(a), the n values measured at 633 nm for the TiO_2, TiO_2-ZrO_2 and ZrO_2 thin films are 1.78, 1.85 and 1.87, respectively. The values of 1.78 for TiO_2 and 1.87 for ZrO_2 is considerably different from the value of 2.49-2.66 for anatase TiO_2 given in a previous report.[17] The value of 1.87 for the ZrO_2 is also different from the value of 2.12 reported for tetragonal ZrO_2 thin film.[18] These lower values are fundamentally attributed to the porosity of the films observed in the FE-SEM inspection, which is mainly due to the volume occupied by the surfactants in the film. The

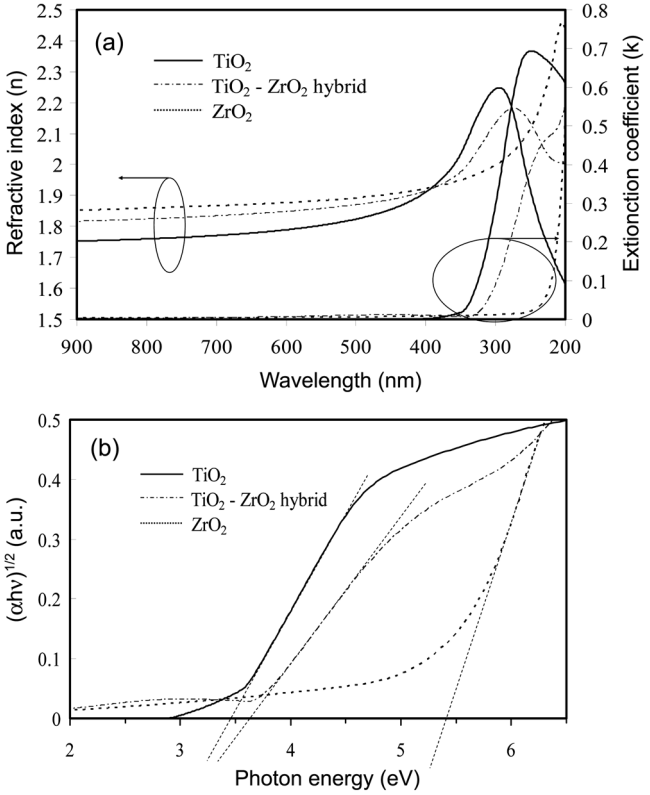

Figure 3. (a) Refractive index (n) and extinction coefficient (k) values by obtained by spectroscopic ellipsometry (b) the Tauc plot of the 450-annealed TiO_2, TiO2-ZrO_2 hybrid, ZrO_2 thin films.

Table 1. Elemental Analysis Data of TiO_2, TiO_2-ZrO_2 hybrid, the ZrO_2 thin films using XPS

	Atomic concentration (%)			
	carbon	oxygen	titanium	zirconium
TiO_2	3	65	32	
TiO_2-ZrO_2 hybrid	3	54	14	29
ZrO_2	5	64		31

relative porosity is calculated from the refractive index values by the Lorenz-Lorentz equation: $P\ (\%) = 1 - [(n_p^2-1)/(n_p^2+2)]/[(n_m^2-1)/(n_m^2+2)]$, where n_m is the refractive index of the matrix film (this could be interpreted as a reference film) and n_p is the refractive index of the porous film.[19] The relative porosity is calculated to be 34-37% for the TiO_2 film and 16% for the ZrO_2 film, by taking the above reference values for TiO_2 and ZrO_2. Here, one concern is that the pore wall structure of the TiO_2 and ZrO_2 films exist as the nanocrystalline domains embedded in amorphous matrix, of which refractive index values could be much different from those of the above references, thereby resulting in different values for the estimated relative porosity.

The Tauc plot obtained from the k values is shown in Figure 3(b), from which the value of the optical band gap is estimated. To derive the Tauc plot from the k values, we need to convert to a values by using the relation $\alpha = 4\pi k/\lambda$. Here, λ is denoted as the wavelength of the incident light. For indirect band gap materials, the inter-band absorption is

summarized by the following equation.[20]

$$\alpha h\nu = (h\nu - E_g)^2$$

The band gap values of the TiO_2, TiO_2-ZrO_2 hybrid, and ZrO_2 films are estimated to 3.43 eV, 3.61 eV, and 5.34 eV, respectively. The band gap value of the TiO_2-ZrO_2 hybrid films is 0.18 eV higher than that of the TiO_2 film. The band gap value of the hybrid film is closer to that of the TiO_2 thin film, than that of ZrO_2. This is quite surprising given that, in the hybrid film, the atomic concentration of zirconium (22%) is much higher than that of titanium (16%) according to the XPS quantification results. At this point, it should be noted that the band gap value can be easily tuned by simply changing the relative concentrations of titanium and zirconium elements.

As shown in the XRD results, the TiO_2 and ZrO_2 thin films have crystallinity in the form of anatase and tetragonal phases, respectively, while observing no crystallinity was observed in the hybrid TiO_2-ZrO_2 thin film. In the hybrid thin film, zirconium atoms replace the sites which were originally occupied by titanium atoms so as to prevent the formation of crystalline TiO_2 domains. Similarly, the titanium atoms prevent the formation of crystalline ZrO_2 domains. In other words, the amorphous character in the TiO_2-ZrO_2 hybrid films provides indirect evidence of the molecular-level mixing of the TiO_2 and ZrO_2 networks. In the precursor solution for the hybrid film, the $Ti(OC_4H_9)_4$ molecules and $Zr(OC_4H_9)_4$ molecules stabilized with acetylacetone ligands simultaneously undergo hydrolysis and condensation to form the sol. It is evident that the titanium and zirconium atoms are homogenously incorporated in the sol state. Meanwhile, the atomic concentration of zirconium is two times higher than that of titanium, as revealed by the XPS results of the hybrid film, although the mole number of the $Ti(OC_4H_9)_4$ molecules is the same as that of the ZBOT molecules during the synthesis of the precursor solution. This is probably because the $Zr(OC_4H_9)_4$ stabilized with acetylacetone ligands has higher reactivity compared to the $Ti(OC_4H_9)_4$ molecules, which is needed to be further studied in the structure-property relationship point of view.

It should be mentioned that the band gap tunability of semiconducting metal oxide thin films has a considerable impact on their application to dye sensitized solar cells (DSSCs). The band gap value means the difference in energy in electron volt units between the energy levels of the conduction band minimum (E_c) and valence band maximum (E_b). Any change in the band gap value is interpreted as either an energy shift of either E_c or E_b. In order to clarify the possibility that the change in the band gap is mainly related to the E_c shift, rather than the E_b shift, we are attempting to investigate the electronic structure of the valence band for the films using photoemission spectroscopy. On the other hand, in the typical DSSC, the ultrafast electron transfer across the dye-TiO_2 interface is believed to be governed by a strong electronic coupling between the exicited state of the adsorbed dye and the conduction band of the TiO_2 nanoparticles.[21] This electronic coupling gives rise to the lifetime broadening of the LUMO of the dye adsorbate, which is denoted by $(h/2\pi)\Gamma$. Here, the electron transfer rate (τ) is obtained from the broadening through the relation $\tau = 658/((h/2\pi)\Gamma)$. At this point, it can be said that any changes in the electronic structure of the TiO_2 such as a change in the band gap, the formation of surface electronic states, etc., have a considerable effect on the electronic coupling at the TiO_2-dye interface, thus varying the electron transfer rate. Therefore, when our TiO_2-ZrO_2 hybrid film with its slightly higher band gap is used as the photoanode material of the DSSC instead of the TiO_2 film, the electron transfer rate at the TiO_2-dye interface must be altered. However, we cannot rule out the possibility that the disappearance of the crystallinity and/or the changes in the local geometry may also have an effect on the electron transfer rate *via.* the modification of the electron coupling mechanism.

Conclusion

We synthesized nanoporous TiO_2-ZrO_2 hybrid films whose band gap could be tuned using a surfactant-templated approach. The TiO_2 and ZrO_2 thin films have anatase and tetragonal crystalline structures, respectively, while the TiO_2-ZrO_2 hybrid film exhibits no crystallinity. This is because the $Ti(OC_4H_9)_4$ and acetylacetone-stabilized $Zr(OC_4H_9)_4$ precursors are mixed at the molecular level to form the sol state. The band gap of the nanoporous TiO_2 is estimated to be 3.43 eV, while that of the TiO_2-ZrO_2 hybrid film was increased to 3.61 eV. To clarify whether this change in the band gap is related to the energy shift of the conduction band minimum (E_c) or valence band maximum (E_b), further studies are needed.

Acknowledgement. This study was financially supported by Chonnam National University.

References

1. Chrysicopoulou, P.; Davazoglou, D.; Trapalis, Chr.; Kordas, G.. *Thin Solid Films* **1998**, *323*, 188.
2. Hoffmann, M. R.; Martin, S. T.; Choi, W.; Bahnemann, D. W. *Chem. Rev.* **1995**, *95*, 69.
3. Smirnova, N.; Gnatyuk, Y.; Eremenko, A.; Kolbasov, G.; Vorobetz, V.; Kolbasova, I.; Linyucheva, O. *Int. J. Photoenergy* **2006**, article ID 85469, pages 1-6.
4. Lien, S. Y.; Wuu, D. S.; Yeh, W. C.; Liu, J. C. *Solar Energy Materials and Solar Cells* **2006**, *90*, 2710-2719.
5. Okuya, M.; Nakade, K.; Kaneko, S. *Solar Energy Materials and Solar Cells* **2002**, *70*, 425.
6. Zukalova, M.; Zukal, A.; Kavan, L.; Nazeeruddin, M. K.; Liska, P.; Grazel, M. *Nano Lett.* **2005**, *5*, 1789.
7. Kim, S. K.; Kim, W. D.; Kim, K. M.; Hwang, C. S.; Jeong, J. *Appl. Phys. Lett.* **2004**, *85*, 4112.
8. Wang, C. W.; Chen, S. F.; Chen, G. T. *J. Appl. Phys.* **2002**, *91*, 9198.
9. Facchetti, A.; Yoon, M. H.; Marks, T. J. *Adv. Mater.* **2005**, *17*, 1705.
10. Wilk, G. D.; Wallace, R. M.; Anthony, J. M. *J. Appl. Phys.* **2001**, *89*, 5243.
11. Tang, J.; Fabbri, J.; Robinson, R. D.; Zhu, Y.; Herman, I. P.;

Steigerwald, M. L.; Brus, L. E. *Chem. Mater.* **2004**, *16*, 1336.
12. Barlage, D.; Arghavani, R.; Dewey, G.; Doczy, M.; Doyle, B.; Kavalieros, J.; Murthy, A.; Roberds, B.; Stokley, P.; Chau, R. *International Electron Devices Meeting*, *Technical Digest*; 2001; pp 10.6.1-10.6.4.
13. Kim, D. J.; Hahn, S. H.; Oh, S. H.; Kim, E. J. *Mater. Lett.* **2002**, *57*, 355-360.
14. Alberius, P. C. A.; Frindell, K. L.; Hayward, R. C.; Kramer, E. J.; Stucky, G. D.; Chmelka, B. F. *Chem. Mater.* **2002**, *14*, 3284.
15. Chi, S. Y.; Marmak, M.; Coombs, N.; Chopra, N.; Ozin, G. A. *Adv. Funct. Mater.* **2004**, *14*, 335.
16. The XPS analysis was conducted after etching the thin films for 800 seconds with an Ar ion gun (energy = 2 KeV), in order to prevent any inaccuracy owing to organic residues adsorbed on the sample surfaces.
17. Diebold, U. *Surf. Sci. Rep.* **2003**, *48*, 53.
18. Aguilar-Frutis, M.; Reyna-Garcia, G.; Garcia-Hipolito, M.; Gyzman-Mendoza, J. *J. Vac. Sci. Technol. A* **2004**, *22*, 1319.
19. Yim, J. H.; Baklanov, M. R.; Gidley, D. W.; Peng, H.; Jeong, H. D.; Pu, L. S. *J. Phys. Chem. B* **2004**, *108*, 8953.
20. Zhu, L. Q.; Fang, Q.; He, G.; Liu, M.; Zhang, L. D. *J. Phys. D: Appl. Phys.* **2006**, *39*, 5285.
21. Lundqvist, M. J.; Nilsing, M.; Persson, P.; Lunell, S. *Int. J. Quantum Chem.* **2006**, *106*, 3214.